RSC Advances

RSC Publishing

COMMUNICATION

View Article Online
View Journal | View Issue

Enhanced emission of $NaYF_4$:Yb,Er/Tm nanoparticles by selective growth of Au and Ag nanoshells†

Cite this: *RSC Advances*, 2013, **3**, 7718

Received 11th September 2012,
Accepted 28th March 2013

DOI: 10.1039/c3ra22130j

www.rsc.org/advances

Palanisamy Kannan,[a] Ferhan Abdul Rahim,[a] Xue Teng,[a] Rui Chen,[b] Handong Sun,[b] Ling Huang[a] and Dong-Hwan Kim*[a]

We report a novel, simple strategy to efficiently enhance the fluorescence of metal-coated up-conversion nanoparticles (UCNPs), $NaYF_4$:Yb,Er/Tm. The UCNPs are functionalized with a polyamidoamine generation 1 (PAMAM G1) dendrimer, followed by a continuous growth of gold (Au) or silver (Ag) nanoshells to selectively enhance the up-converted green, violet and blue emissions (>20 fold).

In recent years, fluoride based up-conversion nanoparticles (UCNPs) have drawn great attention in many biological applications due to their high degree of photostability, low excitation energy, which is less harmful to living organisms, along with the avoidance of autofluorescence, which arises from UV excitation of biological materials.[1–8] Despite such advantages, the application of UCNPs has been limited due to their low emission efficiency (<1%), which results from surface quenching. This is particularly significant in small nanoparticles with a large surface area/volume ratio and a relatively small cross section of photon absorption. Maximizing up-conversion quantum yield, often explored by exploiting optimum combinations of different host matrices and rare-earth atoms,[9,10] is one of the most important, yet challenging, tasks aimed at improving the fluorescence yield.

When optimized to provide an electric field enhancement, the inherent surface plasmon resonance (SPR) of the noble metal nanoparticles can be an efficient promoter of fluorescence, namely metal enhanced fluorescence.[11–13] The origin of plasmonic enhancement can be primarily attributed to two effects: (i) an increase in the excitation rate, which is an enhancement of the effective excitation flux caused by local field enhancement associated with plasmon resonance, and (ii) an increase in the emission rate, which is an enhancement of the emission efficiency due to the coupling of the up-conversion emission with the plasmon resonance in proximity, which effectively increase both the non-radiative and radiative decay rate.[14–19] It has been discovered that, when a fluorophore directly contacts with a metal, its fluorescence is quenched, while the fluorescence can be strongly enhanced with a separation gap of a few nanometers between the fluorophore and the metal.[20]

To this end, layer-by-layer assemblies of polyallylamine, polystyrene sulfonate and trisodium citrate have been used as spacer molecules between the metal shell and the UCNP core to effectively modulate fluorescence enhancement.[21–24] However, the enhancement of the fluorescence was relatively small (less than 8-fold).[23] Recently, Xu *et al.*, and Yuan *et al.* found the fluorescence enhancements of rare-earth nanoparticles are 9.8 and 14.4 fold, respectively, by using Ag nanohybrides/composites.[25,26] We believe that such insignificant enhancement could be attributed to the limited thickness tunability of polymeric spacers, and Au^{3+} ion permeation through the polymeric spacer, which induces quenching.[22,23,27,28] In contrast to commonly used poly-electrolytes, we hypothesize that a polyamidoamine generation 1 (PAMAM G1) dendrimer could be a viable option for the spacer molecule because of its facile, yet precise, thickness controllability, along with the fact that PAMAM is an efficient promoter of fluorescence.[29,30] In this work, we synthesized UCNPs co-doped with both Er and Tm ions ($NaYF_4$:Yb,Er/Tm) to selectively tune the fluorescence spectrum through hetero-integration of an Au and Ag nanoshell structure. The co-doped UCNPs were prepared by a slight modification of Capobianco's method.[31] The surface functionalization and characterization of the UCNPs are described in the ESI† (Fig. S1–S3). A representation of the preparation of our core–shell structured UCNPs are shown in Scheme 1. The continuous growth of Au and Ag nanoshells (Au@$NaYF_4$:Yb,Er/Tm and Ag@$NaYF_4$:Yb,Er/Tm, respectively) was conducted by a seed-mediated growth method after the functionalization of a PAMAM G1 dendrimer on UCNPs. We observed that the Au and Ag nanoshells significantly enhanced the emissions of UCNPs by up to ~22 times at selected wavelengths.

Fig. 1 shows the TEM images of the Au and Ag nanoshells on UCNPs. The Au seeds anchored on the UCNPs surface act as nuclei for Au nanoshell growth *via* a surface catalysed reduction of

[a]*School of Chemical and Biomedical Engineering, Nanyang Technological University, 70 Nanyang Drive, 637457, Singapore. E-mail: dhkim@ntu.edu.sg; Fax: +65 6791 1761; Tel: +65 6316 8825*

[b]*Division of Physics and Applied Physics, School of Physical and Mathematical Sciences, Nanyang Technological University, 21 Nanyang Link, 637371, Singapore*

† Electronic supplementary information (ESI) available: Experimental section and data, as indicated in text. See DOI: 10.1039/c3ra22130j

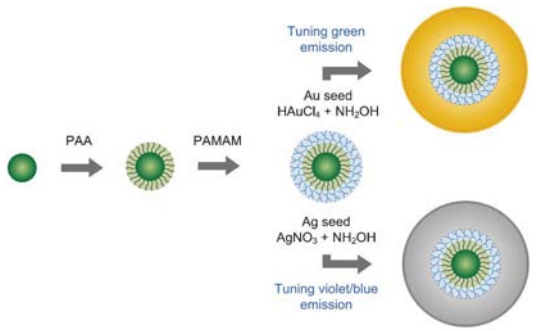

Scheme 1 Schematic representation of the PAMAM G1 templated approach used for the gold and silver nanoshell encapsulation of $NaYF_4$:Yb,Er/Tm UCNPs. PAA: poly-(acrylic acid). PAMAM: polyamidoamine generation 1.

Au^{3+} by hydroxylamine.[32–34] The TEM image of the Au@$NaYF_4$:Yb,Er/Tm core–shell structure shows individual UCNPs with an average size of 53 ± 3 nm in diameter, along with a uniform and smooth Au nanoshell with a thickness of ~20 nm (Fig. 1A and B). The uncoated UCNPs (Fig. S1, ESI†) have an average size of 35 ± 1 nm in diameter. The same protocol was used for the Ag nanoshell growth, which led to the formation of a smooth Ag nanoshell with a thickness of ~20 nm (Fig. 1C and D). The Au nanoshell growth on UCNP was evaluated by selected area electron diffraction pattern analysis. Before Au nanoshell formation, no diffraction pattern is seen in inset "E" of Fig. 1B, whereas after the Au nanoshell growth, characteristic diffraction patterns of gold crystal are identified in inset "F", indicating the presence of (111) crystallographic planes of nanocrystalline Au^0.

X-ray diffraction (XRD) pattern measurements confirmed nanoshell formation. Fig. 2A shows the crystalline structures of $NaYF_4$:Yb,Er/Tm, Au@$NaYF_4$:Yb,Er/Tm and Ag@$NaYF_4$:Yb,Er/Tm.

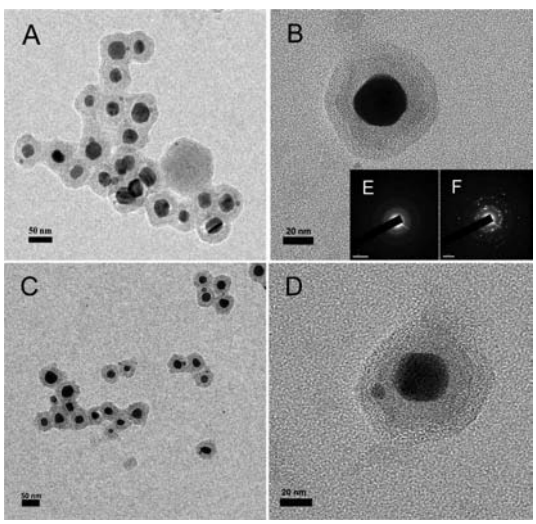

Fig. 1 TEM images of Au (A, B) and Ag (C, D) nanoshells grown on $NaYF_4$:Yb,Er/Tm UCNPs. High resolution TEM images of Au (B) and Ag (D) nanoshells encapsulated single UCNPs. Inset in Image "B": SAED pattern of before (E) and after (F) the growth of the Au nanoshell on UCNPs. Scale bare: A and C: 50 nm, B and D: 20 nm.

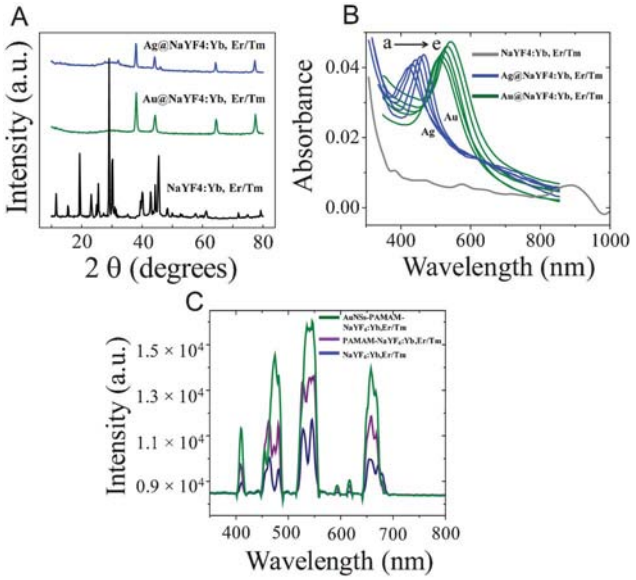

Fig. 2 (A) XRD pattern of bare $NaYF_4$:Yb,Er/Tm NPs (black), after growth of Au (green) and Ag nanoshells (blue) on $NaYF_4$:Yb,Er/Tm nanoparticles. (B) UV-vis spectra of Ag (blue lines) and Au (green lines) nanoshells grown on $NaYF_4$:Yb,Er/Tm NPs. Bare UCNPs is represented by the gray line. UV-vis spectra of both Ag and Au nanoshell growth were measured after 5, 10, 20, 30 and 40 min intervals, as indicated by the arrow (a–e). (C) Fluorescence spectra obtained for $NaYF_4$:Yb,Er/Tm NPs (blue), PAMAM G1 on $NaYF_4$:Yb,Er/Tm NPs (violet) and after assembly of Au seeds on PAMAM G1 self-assembled on $NaYF_4$:Yb,Er/Tm NPs (green).

Peak positions and intensities of the bare UCNPs (black line) are in good agreement with the calculated values for the hexagonal $NaYF_4$ nanocrystal;[35,36] the lattice constant of $NaYF_4$:Yb,Er/Tm is calculated to be 5.31 Å.[7,37] The XRD pattern of Au@$NaYF_4$:Yb,Er/Tm (green line) nanoparticles shows strong diffraction features appearing at 38.20°, 44.41°, 64.54° and 77.50°, corresponding to the (111), (200), (220) and (311) facets of the face-centred cubic crystal structure of Au crystalline facets, respectively. We also observed a similar diffraction pattern for the Ag@$NaYF_4$:Yb,Er/Tm nanoparticles (blue line). Most of the $NaYF_4$:Yb,Er/Tm XRD diffraction peaks diminish upon formation of Au and Ag nanoshells, except a broad shoulder appearing at 27–32°, which is an overlapping region of (110) and (101) peaks.

Metal-enhanced luminescence of UCNPs can be achieved when the absorption or emission band of the luminophores lies in proximity to the surface plasmon band of metal nanoparticles.[38] Therefore, uniform and controlled growth of metallic nanoshells on UCNPs plays a cohesive role in tuning the fluorescent properties of nanoparticles. Fig. 2B presents a series of UV-vis spectra of $NaYF_4$:Yb,Er/Tm, Ag@$NaYF_4$:Yb,Er/Tm and Au@$NaYF_4$:Yb,Er/Tm in an aqueous dispersion. The unmodified UCNPs only have a broad band around 895 nm, indicating the presence of Yb ions (grey line in Fig. 2B). Then, the growth of the Ag nanoshell on $NaYF_4$:Yb, Er/Tm nanoparticles exhibits an absorption peak at ~420 nm, which subsequently red shifts (up to 40 nm) with further growth of the Ag nanoshell (Fig. 2B (blue lines)). This plasmonic resonance frequency of the Ag nanoshell

adequately overlaps with the two major emission peaks, violet and blue, of the $NaYF_4$:Yb, Er/Tm (413 and 452 nm) nanoparticles.

To prove our hypothesis that the PAMAM G1 dendrimer is a suitable spacer molecule between the metal nanoshell and the UCNP core, we explored the emission properties of PAMAM G1-decorated UCNPs (Fig. 2C). The $NaYF_4$:Yb,Er/Tm UCNPs modified with amine-functionalized PAMAM G1 (Fig. 2C, curve b) exhibit an increase in fluorescence, ~1.5 fold higher than PAA–UCNPs (Fig. 2C, curve a). This result shows that the PAMAM acts as a fluorescence enhancer by forming a host–guest inclusion complex of the UCNPs and the PAMAM dendrimer through EDC–NHC coupling.[29,30] Additionally, recent studies reported that PAMAM G1 could act as a fluoro-active relay molecule.[29,30] Well-matched with this previous report, the PAMAM G1 with Au nanoseeds attached to its amine groups shows higher fluorescence intensity (2.1 fold) than PAA–UCNPs (Fig. 2C curve c). Such enhancement is due to the linearly ordered and compact structure of the PAMAM G1 dendrimer, which can (1) avoid the corrosive effect of acidic $HAuCl_4$, and (2) block the diffusion of Au^{3+} to the UCNP core through a spacer, thus minimizing the quenching effect. Taken together, the PAMAM G1 dendrimer can evidently serve as an efficient spacer, separator, and promoter between the metallic shell and the UCNP core.

Fig. 3A depicts the fluorescence spectra at various growth time intervals. The emission spectra of the UCNPs during the Ag nanoshell growth show significant emission intensities at 413 and 452 nm, and an enhancement factor of more than 20 fold was achieved. The surface plasmon resonance of the Ag nanoshell can be effectively coupled with the violet and blue emissions of Tm ions in the UCNPs and enhances the emission, which was calculated to be 20 and 22 times at 413 and 452 nm, respectively, whereas the emission enhancement in the green and red wavelength regions of the same UPNPs is relatively small (~3 times) due to the large coupling distance between the Ag nanoshell and the green/red wavelength. On the other hand, the curves, a–f, in Fig. 3C represent fluorescence spectra at various growth time intervals for the case of the Au nanoshell on the UCNPs. The Au nanoshell growth on UCNPs revealed an absorption peak at 520 nm, and subsequent growth of the Au nanoshell leads to a red-shift of the absorption peak (up to 38 nm) as shown in Fig. 2B (green lines). The emission spectra of the UCNPs during the Au nanoshell growth showed almost the same amount of emission intensity (compared to Ag) at 518 and 540 nm regions. This plasmonic resonance frequency of the Au nanoshell overlaps well with the two adjacent green emission peaks of $NaYF_4$:Yb,Er/Tm (518 and 540 nm) and enhances the emission efficiency by as much as 20 and 21 times for green peaks at 518 and 540 nm, respectively. Low emission enhancement is observed at the violet and blue regions (2.8 times) of the same UCNPs. The evolution of the emission spectra shows the emission intensity beginning to saturate substantially after 30 min of growth of both Ag and Au nanoshells (curve f in Fig. 3A and C). Other research groups have exploited the use of AuNP seeds,[22] Au plasmonic shells,[23] and AgNPs[37] to enhance the emission of UCNPs by up to 2.5, 8 and 10.1-fold, respectively. Compared to previous work, we achieved significant emission improvement in this present study, particularly in the selective region of violet, blue and green emission of the $NaYF_4$:Yb,Er/Tm UCNPs.

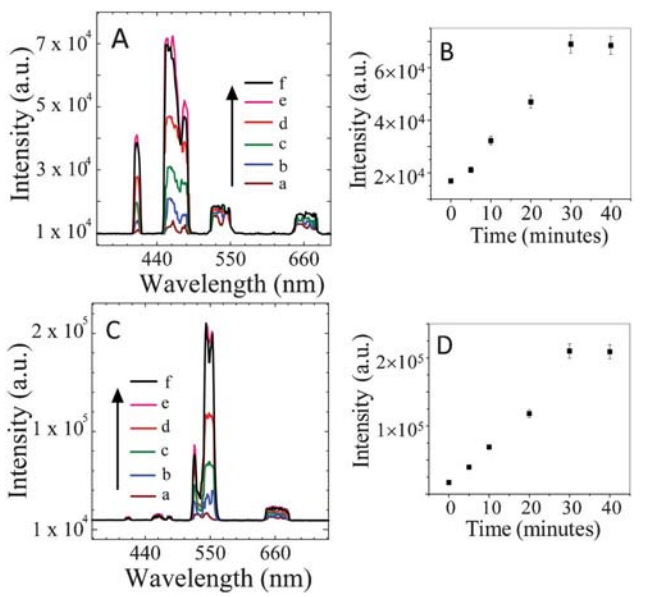

Fig. 3 Fluorescence spectra of $NaYF_4$:Yb,Er/Tm nanoparticles before (a) and after the growth of Ag (A) and Au (C) nanoshells at different growth time intervals (fluorescence spectra a–f corresponding to 0, 5, 10, 20, 30 and 40 min respectively). Plots of the photoluminescence intensity variation against different time intervals of the Ag (B) and Au (D) nanoshell growth (corresponding data were taken from Fig. 3A and C, respectively).

In conclusion, we have prepared a new photonic material with tunable plasmonic and up-converting properties by coating Au and Ag nanoshells on UCNPs, with a PAMAM G1 dendrimer as a spatial spacer and optical promoter. We achieved significant and selective enhancement of up-converted green, violet and blue emission. Our strategy can be used to improve the efficiency of up-conversion nanomaterials and to functionalize nanoparticles for applications in photonic, therapeutic and bioimaging fields.

Acknowledgements

We gratefully acknowledge the financial support from the National Medical Research Council (NMRC/EDG/1060/2012) of Singapore.

References

1 F. Vetrone, R. Naccache, V. Mahalingam, C. G. Morgan and J. A. Capobianco, *Adv. Funct. Mater.*, 2009, **19**, 2924–2929.
2 V. Mahalingam, F. Vetrone, R. Naccache, A. Speghini and J. A. Capobianco, *Adv. Mater.*, 2009, **21**, 4025–4028.
3 J.-C. Boyer, L. A. Cuccia and J. A. Capobianco, *Nano Lett.*, 2007, **7**, 847–852.
4 Z. Chen, H. Chen, H. Hu, M. Yu, F. Li, Q. Zhang, Z. Zhou, T. Yi and C. Huang, *J. Am. Chem. Soc.*, 2008, **130**, 3023–3029.
5 H.-X. Mai, Y.-W. Zhang, R. Si, Z.-G. Yan, L.-d. Sun, L.-P. You and C.-H. Yan, *J. Am. Chem. Soc.*, 2006, **128**, 6426–6436.
6 G.-S. Yi and G.-M. Chow, *Chem. Mater.*, 2006, **19**, 341–343.
7 G. S. Yi and G. M. Chow, *Adv. Funct. Mater.*, 2006, **16**, 2324–2329.

8 H. Schäfer, P. Ptacek, O. Zerzouf and M. Haase, *Adv. Funct. Mater.*, 2008, **18**, 2913–2918.
9 F. Auzel, *Chem. Rev.*, 2003, **104**, 139–174.
10 F. Wang and X. Liu, *Chem. Soc. Rev.*, 2009, **38**, 976–989.
11 J. R. Lakowicz and Y. Fu, *Laser Photonics Rev.*, 2009, **3**, 221–232.
12 F. Tam, G. P. Goodrich, B. R. Johnson and N. J. Halas, *Nano Lett.*, 2007, **7**, 496–501.
13 L. R. Joseph, *Anal. Biochem.*, 2005, **337**, 171–194.
14 W. Feng, L.-D. Sun and C.-H. Yan, *Chem. Commun.*, 2009, 4393–4395.
15 R. Bardhan, N. K. Grady, J. R. Cole, A. Joshi and N. J. Halas, *ACS Nano*, 2009, **3**, 744–752.
16 K. Ray, R. Badugu and J. R. Lakowicz, *J. Am. Chem. Soc.*, 2006, **128**, 8998–8999.
17 S. Schietinger, T. Aichele, H.-Q. Wang, T. Nann and O. Benson, *Nano Lett.*, 2009, **10**, 134–138.
18 P. P. Pompa, L. Martiradonna, A. D. Torre, F. D. Sala, L. Manna, M. De Vittorio, F. Calabi, R. Cingolani and R. Rinaldi, *Nat. Nanotechnol.*, 2006, **1**, 126–130.
19 Y. Chen, K. Munechika and D. S. Ginger, *Nano Lett.*, 2007, **7**, 690–696.
20 K. Sokolov, G. Chumanov and T. M. Cotton, *Anal. Chem.*, 1998, **70**, 3898–3905.
21 A. Tao, P. Sinsermsuksakul and P. Yang, *Nat. Nanotechnol.*, 2007, **2**, 435–440.
22 H. Zhang, Y. Li, I. A. Ivanov, Y. Qu, Y. Huang and X. Duan, *Angew. Chem., Int. Ed.*, 2010, **49**, 2865–2868.
23 L. Sudheendra, V. Ortalan, S. Dey, N. D. Browning and I. M. Kennedy, *Chem. Mater.*, 2011, **23**, 2987–2993.
24 N. Liu, W. Qin, G. Qin, T. Jiang and D. Zhao, *Chem. Commun.*, 2011, **47**, 7671–7673.
25 W. Xu, X. Bai, S. Xu, Y. Zhu, L. Xia and H. Song, *RSC Adv.*, 2012, **2**, 2047–2054.
26 P. Yuan, Y. H. Lee, M. K. Gnanasammandhan, Z. Guan, Y. Zhang and Q.-H. Xu, *Nanoscale*, 2012, **4**, 5132–5137.
27 Y. Jin and X. Gao, *Nat. Nanotechnol.*, 2009, **4**, 571–576.
28 A. Priyam, N. M. Idris and Y. Zhang, *J. Mater. Chem.*, 2012, **22**, 960–965.
29 M. J. Jasmine and E. Prasad, *J. Phys. Chem. B*, 2010, **114**, 7735–7742.
30 N. Stojanovic, L. D. Murphy and B. D. Wagner, *Sensors*, 2010, **10**, 4053–4070.
31 J.-C. Boyer, F. Vetrone, L. A. Cuccia and J. A. Capobianco, *J. Am. Chem. Soc.*, 2006, **128**, 7444–7445.
32 K. R. Brown and M. J. Natan, *Langmuir*, 1998, **14**, 726–728.
33 G. Stremsdoerfer, H. Perrot, J. R. Martin and P. Clechet, *J. Electrochem. Soc.*, 1988, **135**, 2881–2886.
34 L. Wang, J. Bai, Y. Li and Y. Huang, *Angew. Chem., Int. Ed.*, 2008, **47**, 2439–2442.
35 K. N. Reddy, M. A. H. Shareef and N. Pandaraiah, *J. Mater. Sci. Lett.*, 1983, **2**, 83–84.
36 D. M. Roy and R. Roy, *J. Electrochem. Soc.*, 1964, **111**, 421–429.
37 S. Heer, K. Kömpe, H. U. Güdel and M. Haase, *Adv. Mater.*, 2004, **16**, 2102–2105.
38 Y. Chen, K. Munechika, I. J.-L. Plante, A. M. Munro, S. E. Skrabalak, Y. Xia and D. S. Ginger, *Appl. Phys. Lett.*, 2008, **93**, 053106–053103.